0026-895X/08/7302-314–322
MOLECULAR PHARMACOLOGY
U.S. Government work not protected by U.S. copyright
Mol Pharmacol 73:314–322, 2008

Vol. 73, No. 2
39149/3298249
Printed in U.S.A.

Anandamide Inhibition of 5-HT_{3A} Receptors Varies with Receptor Density and Desensitization

Wei Xiong, Masako Hosoi, Bon-Nyeo Koo, and Li Zhang

Laboratory for Integrative Neuroscience, National Institute on Alcohol Abuse and Alcoholism, National Institutes of Health, Bethesda, Maryland 20892, USA

Received June 19, 2007; accepted November 1, 2007

ABSTRACT

Converging evidence has suggested that anandamide (AEA), an endogenous agonist of cannabinoid (CB) receptors, can directly interact with certain types of ligand-gated ion channels (LGICs). However, little is known about the molecular and cellular mechanisms of AEA-induced direct effects on LGICs. Here, we report that AEA inhibited the function of serotonin-gated ion channels (5-HT_{3A}) expressed in *Xenopus laevis* oocytes and human embryonic kidney 293 cells in a manner that was dependent on the steady-state receptor density at the cell surface. The magnitude of AEA inhibition was inversely correlated with the expression levels of receptor protein and function. With increasing surface receptor expression, the magnitude of AEA inhibition decreased. Consistent with this idea, pretreatment with actinomycin D, which inhibits transcription, decreased the amplitude of current activated by maximal concentrations of 5-hydroxytryptamine (5-HT) and increased the magnitude of AEA inhibition. AEA did not significantly alter 5-HT_{3A} receptor trafficking. However, AEA accelerated 5-HT_{3A} receptor desensitization time in a concentration-dependent manner without significantly changing receptor activation and deactivation time. The desensitization time was correlated with the AEA-induced inhibiting effect and mean 5-HT current density. Applications of 5-hydroxyindole and nocodazole, a microtubule disruptor, significantly slowed 5-HT_{3A} receptor desensitization and reduced the magnitude of AEA inhibition. These observations suggest that 5-HT_3 receptor density at the steady state regulates receptor desensitization kinetics and the potency of AEA-induced inhibiting effect on the receptors. The inhibition of 5-HT_3 receptors by AEA may contribute to its physiological roles in control of pain and emesis.

The endocannabinoid anandamide (AEA) is synthesized from lipid precursors in cell membranes via calcium- and G-protein-dependent processes. Rapidly released from neurons after membrane depolarization, AEA can modulate many brain functions by preferentially activating presynaptic cannabinoid type 1 (CB1) receptors (Pacher et al., 2006). However, accumulating evidence has indicated that there are additional molecular sites that may mediate AEA action in the central and peripheral nervous system. AEA has also been found to directly modulate the function of various ligand-gated ion channels (LGICs) such as the serotonin type 3 (5-HT_3) receptors, nicotinic acetylcholine (nACh) α7 and α4β2 subunits and glycine receptors (Fan, 1995; Barann et al., 2002; Oz et al., 2002, 2003; Hejazi et al., 2006; Spivak et al., 2007). Moreover, some AEA-induced behavioral effects are not mediated by activation of CB_1 receptors. For example, AEA can induce catalepsy and analgesia in CB1 knockout mice (Zimmer et al., 1999). AEA has been found to attenuate neuronal excitability and pain via a CB1-independent mechanism in mice (Adams et al., 1998).

5-HT_3 receptors are involved in pain transmission, analgesia, mood disorders, and drug abuse (Zhang and Lummis, 2006). Selective 5-HT_3 receptor antagonists have anxiolytic and antiemetic effects in human and in animal models (Zhang and Lummis, 2006). The levels of 5-HT_{3A} receptors are differentially expressed in brain regions and subpopulations of neurons (Tecott et al., 1993; Morales and Bloom, 1997; Spier et al., 1999; Morales and Wang, 2002). Although high levels of 5-HT_3 receptors are found in nucleus of the tractus solitarius and area postrema, low levels of the receptors are expressed in nucleus accumbens and striatum (Waeber et al., 1988, 1989, 1990; Barnes et al., 1989; Pratt et al., 1990; Tecott et al., 1993; Morales and Bloom, 1997). Overexpression of 5-HT_{3A} receptors in mouse forebrain increases the sensitivity to alcohol-induced behavioral effects

This work was supported by funds from the intramural program of National Institute on Alcohol Abuse and Alcoholism.
Article, publication date, and citation information can be found at http://molpharm.aspetjournals.org.
doi:10.1124/mol.107.039149.

ABBREVIATIONS: AEA, anandamide; CB1, cannabinoid type 1; LGIC, ligand-gated ion channel; 5-HT, 5-hydroxytryptamine; nACh, nicotinic acetylcholine; NG, nodose ganglion; PBS, phosphate-buffered saline; HEK, human embryonic kidney; ANOVA, analysis of variance; 5-HTID, 5-hydroxyindole; NOC, nocodazole; DMSO, dimethyl sulfoxide; AcD, Actinomycin D; MCD, mean current density; BTX, α-bungarotoxin pharmatope; BSA, bovine serum albumin; GR65630, 3-(5-methyl-1*H*-imidazol-4-yl)-1-(1-methylindol-3-yl)propan-1-one; OCB, open channel blocker.

and enhances hippocampal-dependent learning and attention (Engel et al., 1998; Engel and Allan, 1999; Harrell and Allan, 2003). Several naturally occurring polymorphisms in human 5-HT$_{3A}$ receptors can significantly change the levels of receptor expression at cell membrane surfaces (Niesler et al., 2001a; Krzywkowski et al., 2007). These mutations are found to associate with affective disorders, the personality trait of harm avoidance, human face processing and emetogenic sensitivity to anticancer drug-induced side effects such as vomiting and nausea (Niesler et al., 2001a,b; Melke et al., 2003; Iidaka et al., 2005; Krzywkowski, 2006).

Despite evidence showing that AEA can directly modulate a variety of ion channel functions, the molecular and cellular mechanisms of the AEA-induced CB1-independent effects remain elusive. AEA has been shown to inhibit the 5-HT$_{3A}$ receptor-mediated responses in rat nodose ganglion (NG) neurons and in cell lines expressing mouse and human 5-HT$_{3A}$ subunits (Fan, 1995; Barann et al., 2002; Oz et al., 2002). However, the potency of AEA inhibition has been found to vary significantly among different cell lines. Whereas AEA inhibits 5-HT$_3$ responses with an EC$_{50}$ value of 0.19 μM in NG neurons, the EC$_{50}$ value of AEA inhibition is 3.7 μM in *Xenopus laevis* oocytes expressing homomeric 5-HT$_{3A}$ receptors (Fan, 1995; Oz et al., 2002). This discrepancy is unlikely because of different compositions of the 5-HT$_3$ subunits that are expressed in native neurons and in heterologous expression systems because the potency of AEA inhibition of homomeric 5-HT$_{3A}$ receptors is similar to that of native receptors expressed in HEK293 cells and NG neurons (Fan, 1995; Barann et al., 2002; Oz et al., 2002). One alternative explanation is that the discrepancy may arise from different levels of receptor expression. To test this hypothesis, we examined the relationships between the extent of the AEA inhibition of 5-HT$_{3A}$ receptors and receptor density at the cell surface. Our results suggest that the steady-state density of 5-HT$_3$ receptors critically influences on receptor desensitization and the sensitivity of 5-HT$_3$ receptors to AEA-induced inhibiting effect.

Materials and Methods

Preparation of cRNAs and Expression of Receptors. The cDNA clone of the mouse 5-HT$_{3A}$ subunit was provided by Dr. David Julius (University of California, San Francisco, CA). The cDNA clone of the human 5-HT$_{3A}$ subunit was purchased from OriGen, Inc (Rockville, MD). Complementary RNAs (cRNAs) were synthesized in vitro using a mMessage mMachine RNA transcription kit (Ambion Inc., Austin, TX). The quality and sizes of synthesized cRNAs were confirmed by denatured RNA agarose gels. Mature female *X. laevis* frogs were anesthetized by submersion in 0.2% 3-aminobenzoic acid ethyl ester (Sigma, St. Louis, MO). Oocytes were surgically excised and separated. The follicular cell layer of the oocytes was removed by treatment with type A collagenase (Sigma-Aldrich) for 10 min at room temperature. Although the amount of cRNA injected into oocytes varied from 1 to 100 ng, as indicated, the injection volume of diethylpyrocarbonate-treated water was kept in 20 nl throughout the entire experiment. Oocytes were incubated at 19°C in modified Barth's solution: 88 mM NaCl, 1 mM KCl, 2.4 mM $NaHCO_3$, 2.0 mM $CaCl_2$, 0.8 mM $MgSO_4$, and 10 mM HEPES, pH7.4.

***X. laevis* Oocyte Electrophysiological Recording.** After incubation for 2 to 5 days, oocytes were studied at room temperature (20–22°C) in a 90-μl chamber. The oocytes were superfused with modified Barth's solution at a rate of 6 ml/min. Agonists and chemical agents were diluted in the bath solution and applied to the oocytes for a specified time, using a solenoid valve-controlled superfusion system. Membrane currents were recorded by two-electrode voltage-clamp at a holding potential of −70 mV, using a GeneClamp 500 amplifier (Molecular Devices, Sunnyvale, CA). The recording microelectrodes were filled with 3 M KCl and had electrical resistances of 0.5 to 3.0 MΩ. Data were acquired using pClamp 9.1 software (Molecular Devices). Average values are expressed as means ± S.E.

Western Blot of Membrane Surface Proteins. Immediately after treatment with AEA, *X. laevis* oocytes expressing 5-HT$_{3A}$ receptors were washed in PBS and incubated with *N*-hydroxysuccinimide-SS-biotin (Pierce, Rockford, IL) at a concentration of 1.5 mg/ml in phosphate-buffered saline (PBS) for 30 min at 4°C under nonpermeabilizing conditions, as described previously (Hollmann et al., 1994; Lan et al., 2001). The oocytes were then washed and homogenized. The homogenate was centrifuged repeatedly at 1000*g* for 10 min at 4°C until all yolk granules and melanosomes were pelleted. The final supernatant was incubated with 100 μl of neutravidin-linked beads (Pierce) by end-over-end rotation for 2 h at 4°C. The beads were centrifuged and washed extensively to isolate bead-bound proteins. Labeled proteins were eluted from the beads by dithiothreitol-containing SDS-PAGE loading buffer and loaded onto 10% SDS/PAGE. After transfer onto a PVDF membrane (Invitrogen), the surface proteins were blocked with PBS, pH 7.5, containing 0.1% Tween 20 (Sigma) and 5% nonfat powdered milk and then incubated for 1 h with a polyclonal antibody (pAb120, 1:2000) directed to the extracellular N-terminal domain of the 5-HT$_{3A}$ receptor (Spier et al., 1999). The proteins were washed, blotted with a 1:600 dilution of fluorescein-linked anti-rabbit Ig in PBS, and incubated with anti-fluorescein-alkaline phosphatase conjugate (Pierce) at 1:2500 dilution in PBS for 1 h. The proteins detected by ECF substrate (GE Healthcare) were scanned using a Storm Gel and Blot Imaging System with ImageQuant image analysis software (GE Healthcare).

HEK 293 Cell Transfection and Whole Cell Recording. HEK 293 cells were cultured as described previously (Hu et al., 2006). The plasmid cDNA of human 5-HT$_{3A}$ receptors was transfected with SuperFect Transfection kit (QIAGEN, Valencia, CA). The currents were recorded 24 to 48 h after transfection. Cells were lifted and continuously superfused with a solution containing 140 mM NaCl, 5 mM KCl, 1.8 mM $CaCl_2$, 1.2 mM $MgCl_2$, 5 mM glucose, and 10 mM HEPES, pH 7.4, with NaOH; ~340 mOsmol with sucrose). Membrane currents were recorded in the whole-cell configuration using an Axopatch 200B amplifier (Molecular Devices) at 20 to 22°C. Cells were held at −60 mV unless otherwise indicated. Data were acquired using pClamp 9 software (Molecular Devices). Bath solutions were applied through three-barrel square glass tubing (Warner Instrument, Hamden, CT) that had been pulled to a tip diameter of ~200 μm. Drugs were applied through Warner fast-step stepper-motor driven system. The 10 to 90% rise time of the junction potential at whole-cell recording was 4 to 12 ms.

Staining and Imaging of 5-HT$_{3A}$ Receptor α-Bungarotoxin (BTX)-Tag Transfected in HEK 293 Cells. To generate 5-HT$_{3A}$ receptor-BTX-tag, two copies of the sequence 5′-TGGCGGTAC-TACGAGAGCAGCCTGGAGCCCTACCCCGAC-3′ were inserted into both 5′ and 3′ ends of the 5-HT$_{3A}$ subunit subcloned in pCDNA 3.1 (−) using polymerase chain reaction amplification. The 5-HT$_{3A}$-BTX-tag was transfected into HEK 293 cells using Lipofectamine 2000 (Invitrogen, Carlsbad, CA). 24 to 48 h after transfection, living cells were stained with tetramethylrhodamine-BTX at 1 μg/ml (Invitrogen) for 5 min at room temperature. Cells were washed twice with PBS and then incubated with 2 μM AEA for 5 min. Cells were stained with Alexa Fluor 488-BTX at 1 μg/ml for 5 min, washed and fixed with 4% paraformaldehyde. Cells were rinsed with PBS and mounted in a glycerol-based mounting medium. Cells were imaged with a CCD camera attached to a Zeiss Axiovert epifluorescence microscope. The Alexa Fluor 488 was excited at 480/35 nm and the emission of light was collated using a 533/35 emission filter with a 1.3 numerical aperture 100× objective. The tetramethylrhodamine

was excited at 540/25 nm and the emission of light was collected using a 605/55 emission filter.

Data Analysis. Statistical analysis of concentration-response data were performed with the use of the nonlinear curve-fitting program Prism. Data were fit using the Hill equation: $I/I_{max} = 1/[1 + (EC_{50}/[Agonist])^{nH}]$, where I is the current amplitude activated by a given concentration of agonist ([Agonist]), I_{max} is the maximum response of the cell, n_H is the Hill coefficient, and EC_{50} is the concentration eliciting a half-maximal response. Data were statistically compared by the paired t test, or analysis of variance (ANOVA), as noted. Average values are expressed as mean ± S.E.

Kinetic Analysis. Receptor activation rate was induced by 30 μM 5-HT and estimated by measuring the slope of the initial inward component of current between 10 and 30% of the maximal current (10%–30% rise time). Receptor desensitization was induced by prolonging incubation with AEA for 30 s. The deactivation time was recorded for 30 s immediately after a brief application of 1 mM 5-HT for 5 ms. The time constants of deactivation and desensitization were determined by fitting with exponential functions using the Marquardt-Levenberg algorithm in Clampfit. The deactivation and desensitization time constants for 5-HT_3-mediated currents were best fit using a biexponential function when expressed in HEK 293 cells. However, a single exponential function was sufficient to accurately fit the desensitization decays of current activated by 5-HT in the presence of AEA. In this case, fast and slow components were normalized from two components to single component following the equation: $(A_{FAST} \times \tau_{FAST} + A_{SLOW} \times \tau_{SLOW})$, where as τ_{FAST} and τ_{SLOW} were the fast and slow decay time constants, and A_{FAST} and A_{SLOW} were the relative proportion of the fast and slow components.

Chemicals. All chemicals used in preparing the solutions were from Sigma-Aldrich (St. Louis, MO). 5-HT was applied by gravity flow via a micropipette positioned 3 mm from the oocyte. Stock solutions of AEA, 5-hydroxyindole (5-HTID), and nocodazole (NOC) were prepared in dimethyl sulfoxide (DMSO) at a concentration of 10 mM. DMSO alone did not affect 5-HT receptor-mediated current when added at concentrations up 0.2% (v/v), which was twice as high as the most concentrated DMSO used in our experiments.

Results

AEA Inhibition Was Independent of Agonist Concentrations. Consistent with a previous observation (Oz et al., 2002), incubation of AEA (10 μM) for 10 to 20 min produced gradually developing inhibition of 5-HT (1 μM)-induced currents in *X. laevis* oocytes previously injected with 2.5 ng of the mouse 5-HT_{3A} subunit cRNA (Fig. 1A). The AEA-induced inhibition reached a maximum of 86% after a 10-min exposure and was completely reversed 30 min after discontinuation of drug application (Fig. 2B). The inhibition by AEA was concentration-dependent with an EC_{50} value of 239 ± 13 nM and slope value of 0.8 ± 0.16 (Fig. 1C). The effect of 10 μM AEA on 5-HT_{3A} receptors was also studied in the presence of different concentrations of 5-HT. The inhibition by AEA was equipotent at all agonist concentrations (Fig. 1D). The EC_{50} and slope values of the 5-HT-concentration response curves were 1.6 ± 0.05 μM and 1.5 ± 0.2 in the absence of AEA, and 1.9 ± 0.2 μM and 1.8 ± 1.0 in the presence of 10 μM AEA. These values were not significantly different ($p > 0.2$, unpaired t test, $n = 5$).

AEA Inhibition Correlated with Receptor Surface Protein and Function. To examine whether the AEA inhibition depends on surface receptor density, we injected various concentrations (1, 2.5, 10, 25, 50, and 75 ng) of mouse 5-HT_{3A} subunit cRNA into *X. laevis* oocytes. We first measured the surface expression of 5-HT_{3A} receptors in oocytes using Western blots by labeling cell-surface proteins with sulfo-*N*-hydroxysuccinimide-SS-biotin (Lan et al., 2001). Figure 2A reveals a representative Western blot of surface receptor proteins from cells injected with 50, 10, and 1 ng of 5-HT_{3A} receptor cRNA. The amplitude of current activated by 100 μM 5-HT also increased with increasing cRNA injection levels (Fig. 2B). AEA at 10 μM inhibited 5-HT_{3A} receptor-mediated current in a manner that depended on the expression levels of surface receptor protein (Fig. 2, B and C). The magnitude of AEA inhibition was strongest at lower receptor expression levels. For instance, the maximal AEA inhibition was 95% (5 ± 2% of control) in oocytes injected with 2.5 ng of 5-HT_{3A} receptor cRNA, whereas the maximal inhibition was only 25% (75 ± 6% of control) in oocytes injected with 50 ng of 5-HT_{3A} receptor cRNA. These values were significantly different (Fig. 2C; unpaired t test, $p < 0.001$). The EC_{50} values of AEA inhibition differed by nearly 120-fold between oocytes previously injected with 1 and 50 ng of cRNAs (Fig. 2D). For instance, the EC_{50} value for AEA inhibition was 167 ± 12 nM in cells injected with 1 ng of cRNA, whereas the EC_{50} value for AEA inhibition was 20 ± 2 μM in cells injected with 50 ng of cRNA. These values were significantly different (Fig. 2D; $p < 0.001$, unpaired t test, $n = 5$). The magnitude of inhibition produced by 10 μM AEA was strongly correlated with the amount of the cRNA injected into the oocytes (Fig. 3A; $p < 0.0001$), the expression level of the receptor proteins (Fig. 3B; $p < 0.0001$) and the

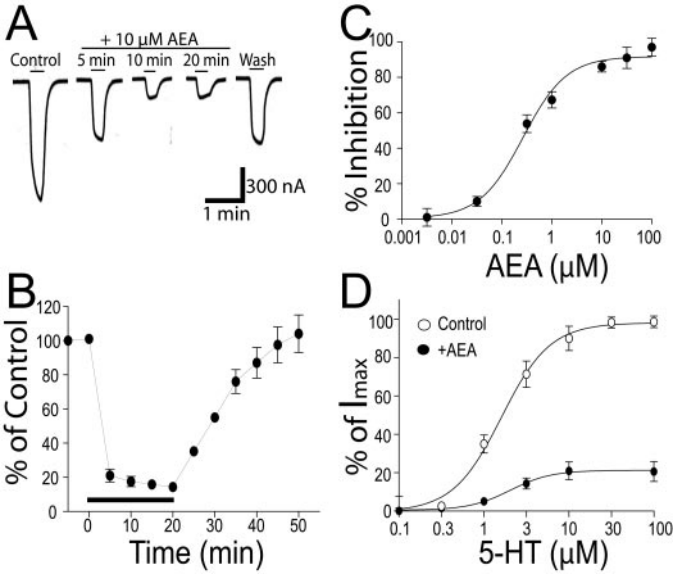

Fig. 1. AEA inhibition of $I_{5\text{-}HT}$ in *X. laevis* oocytes expressing 5-HT_{3A} receptors. A, AEA inhibition of $I_{5\text{-}HT}$. Tracing records showing currents activated by 1 μM 5-HT in the absence and presence of 10 μM AEA. The solid bar on the top of each trace record represents the time of 5-HT application. A long solid bar indicates the time of continuous application of AEA. B, time course of AEA inhibition of $I_{5\text{-}HT}$ in cells previously injected with 2.5 ng of cRNA of mouse 5-HT_{3A} subunit. The solid bar indicates the application time of 10 μM AEA. Each data point represents mean ± S.E. from at least seven oocytes. Error bars are omitted if they were smaller than the size of symbols. C, the concentration-response curve of AEA inhibition of $I_{5\text{-}HT}$ in oocytes previously injected with 2.5 ng of cRNA of the mouse 5-HT_{3A} subunit. The curve is best fit to the Hill equation as described under *Materials and Methods*. Each data point represents mean ± S.E. from at least seven oocytes. D, noncompetitive inhibition of 5-HT_{3A} receptor-mediated responses by AEA. 5-HT concentration-response curves in the absence (○) and in the presence of 10 μM AEA (●).

maximal current activated by 100 μM 5-HT (Fig. 3C; $p = 0.002$).

AcD Increased AEA Inhibition. To further confirm the relationship between receptor density and AEA inhibition, we preincubated oocytes with 10 μg/ml AcD, which inhibits RNA transcription, for 24 h before recordings. We observed that AcD significantly reduced current amplitude activated by 100 μM 5-HT from 7.8 ± 2.5 to 1.4 ± 0.4 μA (Fig. 4A; $p < 0.001$, unpaired t test, $n = 7$). This suggests that AcD can reduce the functional expression of 5-HT$_{3A}$ receptors. On the other hand, AcD significantly increased the magnitude of AEA inhibition from 53 ± 11% to 88 ± 2% (Fig. 4B; $p < 0.02$, unpaired t test, $n = 7$).

AEA Inhibition Correlated with Mean Current Density. The above observations indicate that potency of AEA inhibition of 5-HT$_{3A}$ receptor function depends on receptor steady-state density at the cell surface. However, one can argue if this phenomenon occurs exclusively in *X. laevis* oocytes, where a slow perfusion system is used. To answer this question, we performed whole-cell recordings combined with fast drug perfusion to examine the effect of AEA on the 5-HT$_{3A}$ subunits expressed in HEK 293 cells. In cells transiently expressing 5-HT$_{3A}$ receptors, the amplitude of current activated by maximal 5-HT (100 μM) varied from 0.3 to 7.9 nA, indicating that the levels of receptor expression differ substantially at the surface of individual cells. AEA inhibited current amplitude activated by 30 μM 5-HT. The magnitudes of average percentage inhibition by 0.1 and 1 μM AEA were 58 ± 3% and 92 ± 2%. These data are in line with a previous study (Barann et al., 2000). Similar to the observations in oocyte experiments, HEK cells that exhibited relatively low current amplitudes were more sensitive to AEA than those that exhibited high-current amplitudes (Fig. 5A). We then calculated MCD by plotting maximal 5-HT current amplitude over capacitance of each individual cell. The extent of MCD was inversely correlated with the percentage of AEA inhibition of current peak (Fig. 5B; linear regression, $p < 0.01$, $n = 13$) and current area (Fig. 5C; linear regression, $p < 0.01$, $n = 13$).

AEA Did Not Affect 5-HT$_{3A}$ Receptor Trafficking. The AEA inhibition develops slowly and requires a preincubation of AEA to reach the maximal effect. This observation prompted us to ask whether AEA inhibits 5-HT$_3$ receptors by

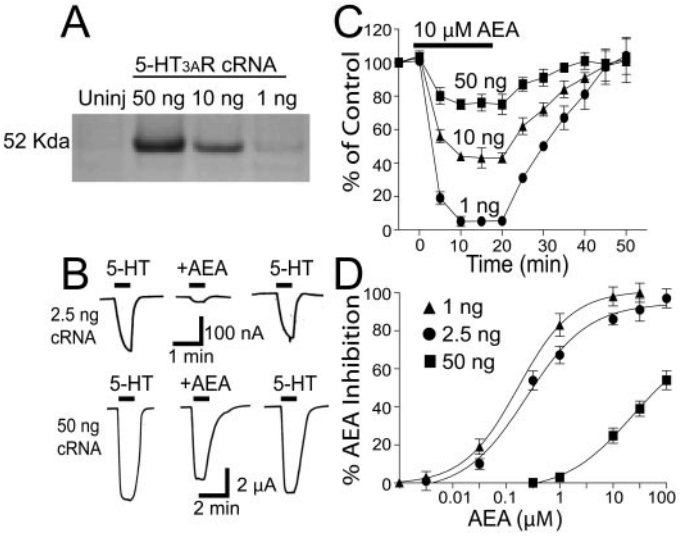

Fig. 2. AEA inhibition depends on expression level of receptor proteins at the cell surface. A, Western blot of 5-HT$_{3A}$ receptor protein at the surface membrane of *X. laevis* oocytes. A representative gel of Western blot showing the abundance of surface proteins from cells previously injected with various concentrations of 5-HT$_{3A}$ receptor cRNAs. B, tracing records showing AEA inhibition of 5-HT-activated currents in cells previously injected with 2.5 ng (top) and 50 ng (bottom) 5-HT$_{3A}$ receptor cRNAs. C, time course of AEA inhibition of $I_{5\text{-}HT}$ in *X. laevis* oocytes previously injected with 1, 20, and 50 ng of the 5-HT$_{3A}$ receptor cRNAs. The solid bar indicates the time of AEA application. Each data point represents mean ± S.E. from the average of five cells. D, concentration-response curves of AEA inhibition of 5-HT-activated current in cells previously injected with 1, 2.5, and 50 ng of 5-HT$_{3A}$ receptor cRNAs. The curves were best fit to the Hill equation as described under *Materials and Methods*. Each data point represents mean ± S.E. from at least 5 oocytes

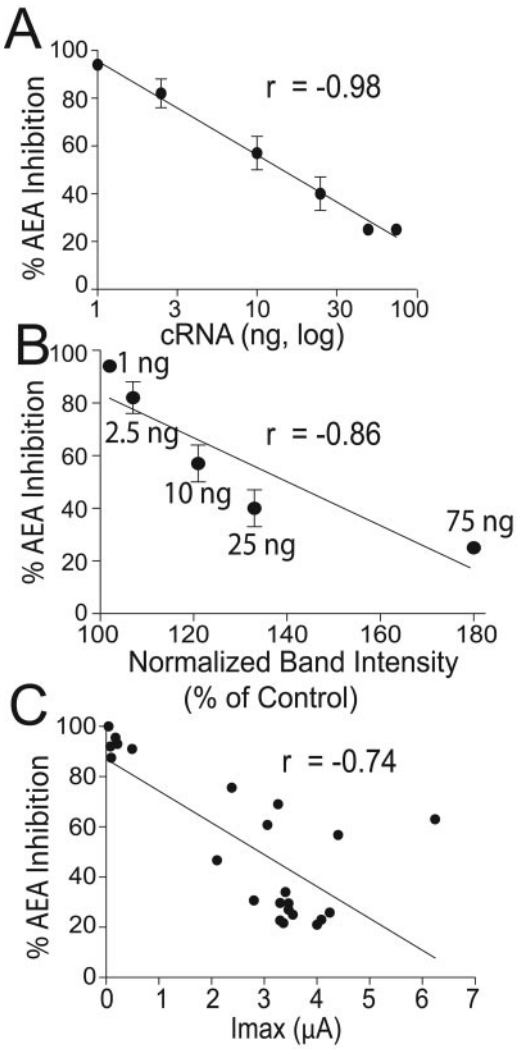

Fig. 3. AEA inhibition correlates with levels of receptor expression. A, correlation between the magnitude of inhibitory effect induced by 10 μM AEA and various concentrations of 5-HT$_{3A}$ receptor cRNAs injected into oocytes (linear regression, $p < 0.0001$, $n = 6$). Each data point represents mean ± S.E. from at least seven oocytes. B, correlation between the magnitude of AEA inhibition and levels of surface 5-HT$_{3A}$ receptor proteins isolated from oocytes previously injected with various concentrations of 5-HT$_{3A}$ receptor cRNA (linear regression, $p < 0.001$, $n = 5$). Each data point represents mean ± S.E. from three separate experiments. The band density was normalized as a percentage of control. C, correlation between the extent of AEA-induced inhibiting effect on 5-HT$_{3A}$ receptors and current amplitude activated by maximal concentration of 5-HT (100 μM) in oocytes previously injected with 1, 10, and 25 ng of 5-HT$_{3A}$ receptor cRNA (linear regression, $p < 0.01$, $n = 24$). These data were collected from the same batch of oocytes.

modulating receptor internalization. We first examined the effect of AEA on 5-HT_{3A} receptor trafficking in living HEK 293 cells that express 5-HT_{3A} receptor proteins tagged on the extracellular amino and carboxyl terminus with a α-bungarotoxin pharmatope (BTX). The 13-amino acid BTX pharmatope is derived from the nACh receptor. The BTX pharmatope-tagged receptors can be labeled by BTX, which allows us to specifically label surface receptors and to visualize receptor trafficking in living cells. Cells were labeled with tetramethylrhodamine-BTX (red) before exposure to AEA and then treated with 2 μM AEA for 5 min. These cells were then labeled with Alexa Fluor-488-BTX (green). Under this experimental procedure, the receptors that were endocytosed during AEA incubation period were observed as red signal within interior of cells. Those Alexa Fluor-488 labeled-receptors that did not enter endocytosis were double-labeled and appeared as yellow signal surround cell perimeter, whereas those that appeared in green may represent newly inserted channels. Figure 6A illustrates double-labeling of 5-HT_{3A} receptors without and with 2 μM AEA. The majority of the 5-HT_{3A} receptors that were on the cell's surface during the initial period had been endocytosed in the absence and presence of AEA. Next, we used a protein biotinylation-labeling method to quantitatively evaluate surface expression of 5-HT_{3A} receptor proteins. The density of the surface protein revealed by Western blot seemed to be similar before and 5, 10, and 20 min after AEA administration (Fig. 6B). The average values of protein gel intensity measured were 97 $\pm$ 10%, 110 $\pm$ 14%, and 104 $\pm$ 12% of control (Fig. 6C). These values were not significantly different (Fig. 6C; $p > 0.5$, ANOVA).

AEA Accelerated Receptor Desensitization. To explore the mechanisms that underlie AEA inhibition of 5-HT_{3A} receptors, we conducted kinetic analysis using fast drug perfusion. Although AEA did not significantly alter the 10% to 30% rise time of 5-HT-activated currents (2.9 $\pm$ 0.1 versus 3.1 $\pm$ 0.1 ms, unpaired t test, $p = 0.2$), AEA seemed to accelerate the desensitization decay of 5-HT-activated current (Fig. 7A) in the prolonged presence of 5-HT ("desensitization"). To properly evaluate the desensitization kinetics, we normalized the fast and slow components using the weighted sum formula described under *Materials and Methods*. We first examined the effect of AEA on the time courses of 5-HT-activated current (●) and receptor desensitization (○). Both AEA-induced inhibition and desensitization developed in similar time courses. However, the receptor desensitization reached the maximal extent after preincubation of AEA for 2 min, whereas the maximal extent of AEA inhibition required 5 min (Fig. 7B). The weighted sum of the desensitization time constant components for 5-HT alone was 536 $\pm$ 87 ms, whereas the weighted sum of the desensitization time constants in the presence of 0.03 and 0.1 μM AEA were 386 $\pm$ 68 and 76 $\pm$ 17 ms, respectively. These values were significantly different from that of control (Fig. 7C; $p <$ 0.01, ANOVA). In contrast, AEA did not significantly affect the deactivation time course, which was also best fit by a biexponential function. The deactivation time constants of the fast decay component averaged 0.12 $\pm$ 0.01 and 0.13 $\pm$ 0.01 s with and without AEA, respectively. The deactivation

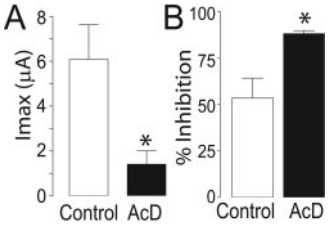

Fig. 4. AcD treatment decreases $I_{5\text{-HT}}$ and increases AEA inhibition of 5-HT_{3A} receptors. A, bar graphs of average amplitude of current induced by maximal concentration of 5-HT (100 μM) without and with AcD treatment of *X. laevis* oocytes expressing mouse 5-HT_{3A} receptors. B, bar graphs represent average percentage of AEA inhibition of 5-HT_{3A} receptors without and with AcD treatment. Each data point represents mean $\pm$ S.E. from five cells. $*$ indicates a significant difference compared with control ($p < 0.02$).

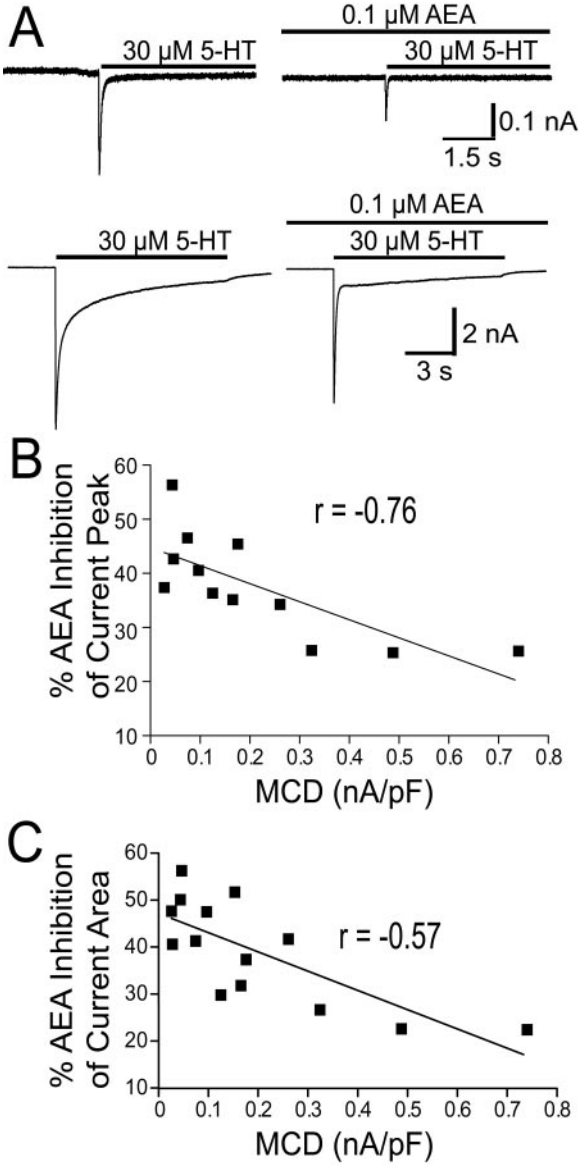

Fig. 5. AEA inhibition correlates with 5-HT_{3A} receptor density expressed in HEK 293 cells. A, representative current records show low- and high-density currents induced by 30 μM 5-HT in the absence and presence of 0.1 μM AEA in HEK 293 cells transiently transfected with the cDNA of human 5-HT_{3A} receptors. AEA was preapplied to a cell for 2 min before application of 5-HT. B, correlation between the percentage AEA inhibition of current amplitude and MCD (linear regression, $p < 0.01$, $n = 12$). C, correlation between the percentage AEA inhibition of current area and MCD (linear regression, $p < 0.01$, $n = 12$).

time constants of the slow component averaged 1.9 ± 0.1 and 1.6 ± 0.2 s in the absence and presence of AEA, respectively. These values were not significantly different ($p > 0.2$, unpaired t test, $n = 12$). A previous study showed that AEA bound to bovine serum albumin (BSA) (Bojesen and Hansen, 2003). A recent study has reported that BSA can accelerate the recovery time of AEA inhibition of nAChα4β2 subunits (Spivak et al., 2007). In view of these findings, we applied 0.3% of BSA during washout time of AEA-induced inhibition. We observed that BSA accelerated the recovery time after AEA inhibition. For instance, the average recovery rates of $I_{5\text{-HT}}$ after AEA inhibition were 42 ± 3 and 59 ± 6% of control current without and with BSA 2 min after AEA application. These values were significant different ($p < 0.01$, unpaired t test, $n = 6$).

Receptor Desensitization Was Correlated with MCD. The above observations suggest that AEA accelerates receptor desensitization. Given the observation that MCD was correlated with AEA inhibition, we predicted that MCD would also correlate with receptor desensitization. This was proved to be the case when a strong correlation was observed between MCD and desensitization time (Fig. 8A; linear regression, $p < 0.001$). MCD was also correlated with percentage inhibition by AEA (Fig. 8B; linear regression, $p < 0.001$, $n = 15$). However, no significant correlation was observed between receptor activation/deactivation and MCD (Fig. 8, C and D; $p > 0.5$, $n = 15$).

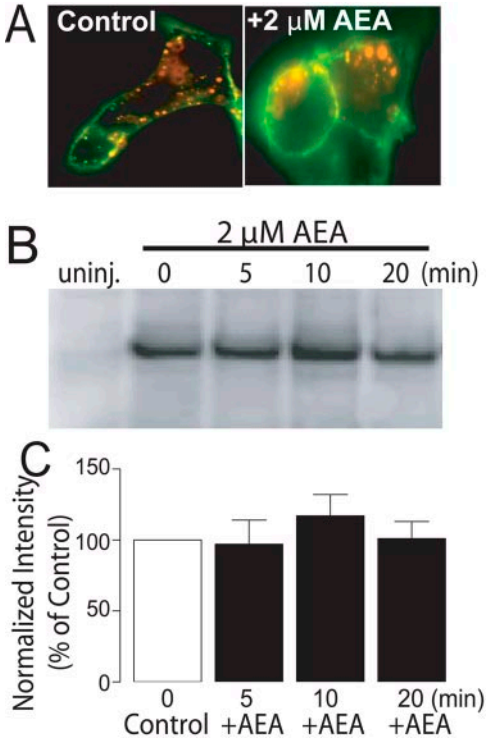

Fig. 6. AEA does not alter receptor trafficking. A, imaging of live HEK 293 cells expressing 5-HT$_{3A}$ receptor-BTX in the absence and presence of 2 μM AEA. Alexa Fluor 488-BTX was first incubated with a cell before 2 μM AEA in *red*. The cell was labeled with a secondary staining of tetramethylrhodamine-BTX after AEA in green. B, a representative Western blot of 5-HT$_{3A}$ receptor surface proteins expressed in *X. laevis* oocytes. C, *bar graphs* represent normalized gel intensity (percentage of control) of 5-HT$_{3A}$ receptor proteins isolated from cell surface of oocytes in the absence (control) and presence of 2 μM AEA. Each data point represents mean ± S.E. from at least three separate experiments.

5-HTID and NOC Slowed Receptor Desensitization and Reduced AEA-Induced Inhibiting Effect on 5-HT$_{3A}$ Receptors. To further explore the mechanism of AEA inhibition, we designed the following experiments. First, we pretreated cells with 25 μM NOC, a microtubule disruptor, for 4 h before electrophysiological recording of 5-HT-activated current. A recent study from our laboratory has shown that disruption of microtubule by NOC can significantly slow mouse 5-HT$_3$ receptor desensitization (Emerit et al., 2005). Consistent with this study, NOC treatment slowed the decay of 5-HT-activated current in HEK 293 cells expressing human 5-HT$_{3A}$ receptors (Fig. 9A). Another approach we used was 5-HTID, which has been shown to slow 5-HT$_3$ receptor desensitization (van Hooft et al., 1997; Gunthorpe and Lummis, 1999). Simultaneous application of 5-HTID at 5 mM

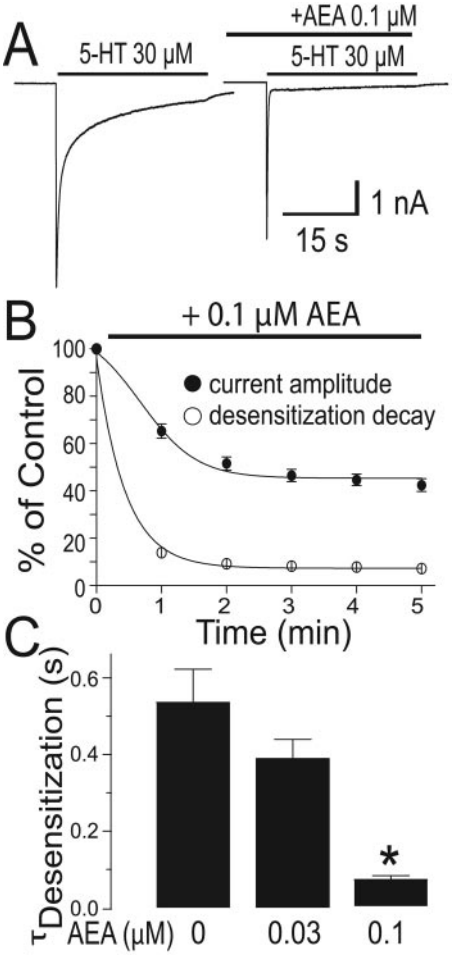

Fig. 7. AEA accelerates receptor desensitization kinetics. A, tracings of 5-HT-activated currents without and with 0.1 μM AEA recorded from a HEK 293 cell expressing human 5-HT$_{3A}$ receptors. The amplitude of current in the presence of AEA was normalized. B, the effect of AEA on the time courses of 5-HT-activated current and receptor desensitization. On the graph, ● indicates average percentage 5-HT current amplitude (during AEA incubation) as average percentage of control (amplitude of 5-HT current before AEA); ○ indicates desensitization time during AEA incubation as average percentage of control (desensitization time before AEA). Each data point represents mean ± S.E. from five individual HEK 293 cells. C, bar graphs represent the average desensitization time of fast components (left) with and without 0.1 μM AEA. Bar graphs (right) represent the sums of fast and slow components of 5-HT$_{3A}$ receptor kinetics without and with AEA. Each data point represents mean ± S.E. from 11 HEK 293 cells. * indicates a significant difference compared with control ($p < 0.001$).

with 5-HT slowed the decay of 5-HT-activated current (Fig. 9A). Pretreatment of HEK 293 cells with NOC and 5-HTID slowed 5-HT_{3A} receptor desensitization time by ~6-fold (solid bars) and, on the other hand, significantly reduced the average percentage of AEA inhibition from 54 ± 3% (control) to 33 ± 2% and 27 ± 6% (Fig. 9B; open bars). These values were significantly different ($p < 0.01$, ANOVA, $n = 11$). The MCD induced by maximal concentration of 5-HT were 0.22 ± 0.04, 0.26 ± 0.05, and 0.18 ± 0.04 nA/pF in the absence (control) and presence of NOC and 5-HTID (Fig. 9C). These values were not significantly different (ANOVA, $p > 0.2$, $n = 14–22$).

Discussion

Our data presented in this study indicate that the sensitivity of 5-HT_3 receptors to AEA-induced inhibiting effect depends on steady-state receptor density at the cell surface. We have shown that surface protein and functional expression of the 5-HT_{3A} receptors were correlated with the extent of AEA inhibition in *X. laevis* oocyte and HEK 293 cells expressing 5-HT_{3A} receptors. A reduction in the functional expression of 5-HT_{3A} receptors induced by AcD treatment increased the sensitivity of 5-HT_{3A} receptors to AEA-induced inhibition. It should be noted that the correlation observed in *X. laevis* oocytes was more dramatic than that of HEK 293 cells. This difference exists because the expression levels of 5-HT_{3A} receptor protein can be readily manipulated in *X. laevis* oocytes. For instance, we injected oocytes with various concentrations of cRNA over a range from 1 to 75 ng. As a result, we observed a difference in the maximal current amplitudes by nearly 350-fold (200–7000 nA). However, the difference of the maximal current amplitude was only 10-fold (200–7000 pA) in HEK 293 cells transiently transfected with 5-HT_{3A} receptor cDNA.

Our results also suggest that receptor density contributes to receptor desensitization, which is the key factor determining the sensitivity of 5-HT_{3A} receptors to AEA-induced inhibition. This is evidenced by our observation that both NOC and 5-HTID reduced both receptor desensitization and AEA inhibition without significantly changing maximal 5-HT current amplitude. We propose that the low-density 5-HT_{3A} receptors at the cell surface should be more efficient than the high-density receptors to enter the desensitized state when exposed to agonist or agonist plus AEA. This idea is supported by a recent study from our laboratory that 5-HT_{3A} receptor desensitization is regulated by the light chain of the microtubule-associated protein 1B (LC1) (Emerit et al., 2005). In this case, MAP1B-LC1 reduces steady state receptor density at the cell surface and accelerates receptor desensitization kinetics at the steady state. Consistent with our

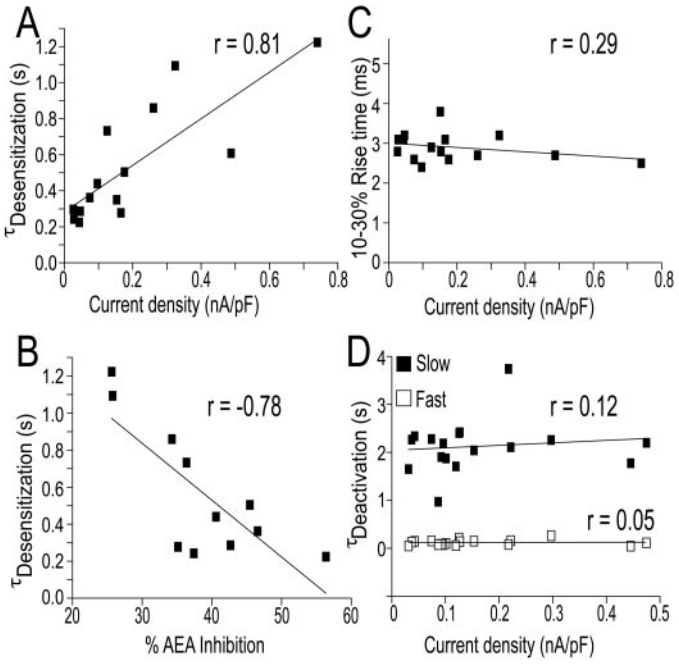

Fig. 8. Receptor desensitization correlates with MCD and AEA inhibition. A, correlation between 5-HT MCD and receptor desensitization time (linear regression, $p < 0.01$). B, correlation between average percentage AEA inhibition and receptor desensitization time (linear regression, $p < 0.01$). C, correlation analysis of 5-HT MCD and receptor activation time (linear regression, $p = 0.4$). D, correlation analysis of 5-HT MCD and the fast (■) and slow (□) components of receptor deactivation kinetics (linear regression, $p = 0.5$).

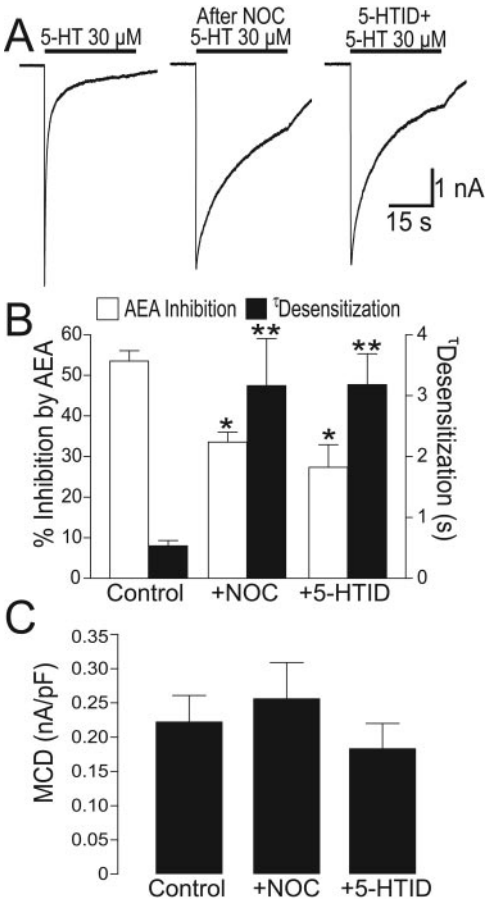

Fig. 9. The effects of NOC and 5-HTID on receptor desensitization and AEA inhibition. A, tracings of 5-HT-activated currents without and with NOC and 5-HTID in HEK 293 cells expressing human 5-HT_{3A} receptors. Cells were pretreated with 25 μM NOC for 4 h and washed thoroughly by perfusion solution during the recording. 5-HTID was applied with 5-HT simultaneously. B, the open bars represent the average percentage inhibition induced by 0.1 μM AEA. The solid bars represent average desensitization time with and without 0.1 μM AEA. The average time constant of receptor desensitization is the sum of fast and slow components of 5-HT_{3A} receptor kinetics without and with AEA. Each data point represents mean ± S.E. from 11 cells. * indicates a significant difference compared with control ($p < 0.02$). ** indicates a significant difference compared with control ($p < 0.001$). C, bar graphs of the calculated MCD in the absence and presence of NOC and 5-HTID. Each data point represents mean ± S.E. from 14 to 22 cells

hypothesis, the steady state density of $GABA_A$ receptors at the cell surfaces has also been found to critically regulate receptor desensitization (Chen et al., 2000; Petrini et al., 2003; Boileau et al., 2005). Likewise, there is a study showing that desensitization of glycine receptors varies with receptor density (Legendre et al., 2002). It should be pointed out that, in addition to receptor density, many other factors contribute to receptor desensitization. These physiological modulators include external calcium concentration (Hu and Lovinger, 2005), post-translational modification of the receptor protein (Yakel and Jackson, 1988) and subunit composition (Hapfelmeier et al., 2003). Future experiments are awaited to determine how the factors listed above regulate AEA-induced inhibiting effect on 5-HT$_3$ receptors.

AEA seems to selectively alter 5-HT$_{3A}$ receptor desensitization kinetics without changing activation and deactivation kinetic properties. This observation is consistent with a previous study showing that AEA does not alter the specific binding of the 5-HT$_3$ receptor antagonist [^{3}H]GR65630 in HEK 293 cells expressing 5-HT$_{3A}$ receptors (Barann et al., 2002). AEA belongs to a group of signaling lipids that can bind proteins through a hydrogen-bonding-like interaction (Bojesen and Hansen, 2003). It is plausible to predict that AEA reduces current amplitude by lowering the energy barrier for receptors to enter a desensitized state. Conversely, 5-HT$_{3A}$ receptor density at the steady state contributes to the free energy barrier required for conformational changes during a receptor desensitization process. It should be pointed out that AEA is unlikely to be an open channel blocker (OCB) at 5-HT$_3$ receptors for the following reasons. First, the inhibitory effect of AEA on 5-HT$_{3A}$ receptors was not voltage-dependent (Fan, 1995; Oz et al., 2002). Second, AEA accelerated receptor desensitization in a concentration dependent manner, whereas a typical OCB usually slows receptor desensitization with increasing its concentrations. Third, AEA became less potent to inhibit 5-HT$_{3A}$ receptors when receptor desensitization was slowed after NOC and 5-HTID treatment, whereas an OCB should be more potent to act at a receptor when its desensitization slows.

LGICs constantly move in and out of synaptic membrane surfaces under various physiological and pathological conditions (Moss and Smart, 2001). Such dynamic receptor trafficking is essential for synaptic transmission and plasticity (Sheng and Pak, 2000). Multiple factors can contribute to the regulation of receptor density at synaptic membrane surfaces. Expression levels of 5-HT$_{3A}$ receptors can be mediated through mechanisms that involve activation of protein kinases (Sun et al., 2003), cytoskeleton proteins (Emerit et al., 2005), naturally occurring genetic variants (Niesler et al., 2001a) and abused drugs such as alcohol (Ciccocioppo et al., 1998). In addition, the expression of these receptors is increased in serotonin transporter deficient mice, suggesting that the extracellular concentration of 5-HT may also influence receptor density (Mössner et al., 2004). Cannabinoids and endocannabinoids exert (in addition to psychotropic effects) strong antinociceptive and antiemetic effects (Pacher et al., 2006). Coincidentally, selective 5-HT$_3$ receptor antagonists are also known to effectively control pain and emesis (Zhang and Lummis, 2006). It should be interesting for future studies to determine the physiological and therapeutic significance of AEA inhibition of 5-HT$_3$ receptors in human and animal models.

We conclude that 5-HT$_3$ receptor steady-state density determines receptor desensitization kinetics and the sensitivity of the receptor to the inhibitory effect of AEA. Such a mechanism seems to account for the variability in AEA inhibition of 5-HT$_3$ receptors expressed in different neurons and cell lines. This mechanism could also be applicable to the inhibitory effect of AEA on the other members of LGICs such as nACh and glycine receptors because AEA has been found to accelerate receptor desensitization kinetics in a manner similar to that observed in 5-HT$_3$ receptors (Lozovaya et al., 2005; Spivak et al., 2007).

Acknowledgments

We thank Drs. David Julius (University of California at San Francisco, San Francisco, CA) and Sarah S. C. Lummis (Cambridge University, Cambridge, UK) for kindly providing the cDNA clones of mouse 5-HT$_3$ receptor and polyclonal 5-HT$_{3A}$ receptor antiserum. We thank Dr. David M. Lovinger for comments on the manuscript. We also thank Guoxiang Lou for constructing 5-HT$_{3A}$R-BTX.

References

Adams IB, Compton DR, and Martin BR (1998) Assessment of anandamide interaction with the cannabinoid brain receptor: SR 141716A antagonism studies in mice and autoradiographic analysis of receptor binding in rat brain. *J Pharmacol Exp Ther* **284:**1209–1217.

Barann M, Meder W, Dorner Z, Bruss M, Bonisch H, Gothert M, and Urban BW (2000) Recombinant human 5-HT3A receptors in outside-out patches of HEK 293 cells: basic properties and barbiturate effects. *Naunyn Schmiedebergs Arch Pharmacol* **362:**255–265.

Barann M, Molderings G, Bruss M, Bonisch H, Urban BW, and Gothert M (2002) Direct inhibition by cannabinoids of human 5-HT3A receptors: probable involvement of an allosteric modulatory site. *Br J Pharmacol* **137:**589–596.

Barnes JM, Barnes NM, Costall B, Ironside JW, and Naylor RJ (1989) Identification and characterisation of 5-hydroxytryptamine 3 recognition sites in human brain tissue. *J Neurochem* **53:**1787–1793.

Boileau AJ, Pearce RA, and Czajkowski C (2005) Tandem subunits effectively constrain GABAA receptor stoichiometry and recapitulate receptor kinetics but are insensitive to GABAA receptor-associated protein. *J Neurosci* **25:**11219–11230.

Bojesen IN and Hansen HS (2003) Binding of anandamide to bovine serum albumin. *J Lipid Res* **44:**1790–1794.

Chen L, Wang H, Vicini S, and Olsen RW (2000) The gamma-aminobutyric acid type A (GABAA) receptor-associated protein (GABARAP) promotes GABAA receptor clustering and modulates the channel kinetics. *Proc Natl Acad Sci U S A* **97:**11557–11562.

Ciccocioppo R, Ge J, Barnes NM, and Cooper SJ (1998) Central 5-HT3 receptors in P and in AA alcohol-preferring rats: An autoradiographic study. *Brain Res Bull* **46:**311–315.

Emerit MB, Sun H, Hu X-Q, Schoenebeck JC, Peoples RW, Miko A, Williams CK, and Zhang L (2005) 5-HT3 receptor linkage to cytoskeleton by MAP1B determines receptor desensitization kinetics. *Soc Neurosci Abstr* **31:**844.17.

Engel SR and Allan AM (1999) 5-HT3 receptor over-expression enhances ethanol sensitivity in mice. *Psychopharmacology (Berl)* **144:**411–415.

Engel SR, Lyons CR, and Allan AM (1998) 5-HT3 receptor over-expression decreases ethanol self administration in transgenic mice. *Psychopharmacology (Berl)* **140:**243–248.

Fan P (1995) Cannabinoid agonists inhibit the activation of 5-HT3 receptors in rat nodose ganglion neurons. *J Neurophysiol* **73:**907–910.

Gunthorpe MJ and Lummis SC (1999) Diltiazem causes open channel block of recombinant 5-HT3 receptors. *J Physiol* **519:**713–722.

Hapfelmeier G, Tredt C, Haseneder R, Zieglgansberger W, Eisensamer B, Rupprecht R, and Rammes G (2003) Co-expression of the 5-HT3B serotonin receptor subunit alters the biophysics of the 5-HT3 receptor. *Biophys J* **84:**1720–1733.

Harrell AV and Allan AM (2003) Improvements in hippocampal-dependent learning and decremental attention in 5-HT(3) receptor overexpressing mice. *Learn Mem* **10:**410–419.

Hejazi N, Zhou C, Oz M, Sun H, Ye JH, and Zhang L (2006) 32 Δ^9-Tetrahydrocannabinol and endogenous cannabinoid anandamide directly potentiate the function of glycine receptors. *Mol Pharmacol* **69:**991–997.

Hollmann M, Maron C, and Heinemann S (1994) *N*-Glycosylation site tagging suggests a three transmembrane domain topology for the glutamate receptor GluR1. *Neuron* **13:**1331–1343.

Hu XQ and Lovinger DM (2005) Role of aspartate 298 in mouse 5-HT3A receptor gating and modulation by extracellular Ca^{2+}. *J Physiol* **568:**381–396.

Hu XQ, Sun H, Peoples RW, Hong R, and Zhang L (2006) An interaction involving an arginine residue in the cytoplasmic domain of the 5-HT3A receptor contributes to receptor desensitization mechanism. *J Biol Chem* **281:**21781–21788.

Iidaka T, Ozaki N, Matsumoto A, Nogawa J, Kinoshita Y, Suzuki T, Iwata N, Yamamoto Y, Okada T, and Sadato N (2005) A variant C178T in the regulatory region of the serotonin receptor gene HTR3A modulates neural activation in the human amygdala. *J Neurosci* **25:**6460–6466.

Krzywkowski K (2006) Do polymorphisms in the human 5-HT3 genes contribute to pathological phenotypes? *Biochem Soc Trans* **34:**872–876.
Krzywkowski K, Jensen AA, Connolly CN, and Brauner-Osborne H (2007) Naturally occurring variations in the human 5-HT3A gene profoundly impact 5-HT3 receptor function and expression. *Pharmacogenet Genomics* **17:**255–266.
Lan JY, Skeberdis VA, Jover T, Grooms SY, Lin Y, Araneda RC, Zheng X, Bennett MV, and Zukin RS (2001) Protein kinase C modulates NMDA receptor trafficking and gating. *Nat Neurosci* **4:**382–390.
Legendre P, Muller E, Badiu CI, Meier J, Vannier C, and Triller A (2002) Desensitization of homomeric alpha1 glycine receptor increases with receptor density. *Mol Pharmacol* **62:**817–827.
Lozovaya N, Yatsenko N, Beketov A, Tsintsadze T, and Burnashev N (2005) Glycine receptors in CNS neurons as a target for nonretrograde action of cannabinoids. *J Neurosci* **25:**7499–7506.
Melke J, Westberg L, Nilsson S, Landen M, Soderstrom H, Baghaei F, Rosmond R, Holm G, Bjorntorp P, Nilsson LG, et al. (2003) A polymorphism in the serotonin receptor 3A (HTR3A) gene and its association with harm avoidance in women. *Arch Gen Psychiatry* **60:**1017–1023.
Morales M and Bloom FE (1997) The 5-HT3 receptor is present in different subpopulations of GABAergic neurons in the rat telencephalon. *J Neurosci* **17:**3157–3167.
Morales M and Wang SD (2002) Differential composition of 5-hydroxytryptamine3 receptors synthesized in the rat CNS and peripheral nervous system. *J Neurosci* **22:**6732–6741.
Moss SJ and Smart TG (2001) Constructing inhibitory synapses. *Nat Rev Neurosci* **2:**240–250.
Mössner R, Schmitt A, Hennig T, Benninghoff J, Gerlach M, Riederer P, Deckert J, and Lesch KP (2004) Quantitation of 5HT3 receptors in forebrain of serotonin transporter deficient mice. *J Neural Transm* **111:**27–35.
Niesler B, Flohr T, Nothen MM, Fischer C, Rietschel M, Franzek E, Albus M, Propping P, and Rappold GA (2001a) Association between the 5′ UTR variant C178T of the serotonin receptor gene HTR3A and bipolar affective disorder. *Pharmacogenetics* **11:**471–475.
Niesler B, Weiss B, Fischer C, Nothen MM, Propping P, Bondy B, Rietschel M, Maier W, Albus M, Franzek E, et al. (2001b) Serotonin receptor gene HTR3A variants in schizophrenic and bipolar affective patients. *Pharmacogenetics* **11:**21–27.
Oz M, Ravindran A, Diaz-Ruiz O, Zhang L, and Morales M (2003) The endogenous cannabinoid anandamide inhibits α_7 nicotinic acetylcholine receptor-mediated responses in *Xenopus* oocytes. *J Pharmacol Exp Ther* **306:**1003–1010.
Oz M, Zhang L, and Morales M (2002) Endogenous cannabinoid, anandamide, acts as a noncompetitive inhibitor on 5-HT3 receptor-mediated responses in Xenopus oocytes. *Synapse* **46:**150–156.
Pacher P, Batkai S, and Kunos G (2006) The endocannabinoid system as an emerging target of pharmacotherapy. *Pharmacol Rev* **58:**389–462.
Petrini EM, Zacchi P, Barberis A, Mozrzymas JW, and Cherubini E (2003) Declusterization of GABAA receptors affects the kinetic properties of GABAergic currents in cultured hippocampal neurons. *J Biol Chem* **278:**16271–16279.
Pratt GD, Bowery NG, Kilpatrick GJ, Leslie RA, Barnes NM, Naylor RJ, Jones BJ, Nelson DR, Palacids JM, Slater P, et al. (1990) Consensus meeting agrees distribution of 5-HT3 receptors in mammalian hindbrain. *Trends Pharmacol Sci* **11:**135–137.
Sheng M and Pak DT (2000) Ligand-gated ion channel interactions with cytoskeletal and signaling proteins. *Annu Rev Physiol* **62:**755–778.
Spier AD, Wotherspoon G, Nayak SV, Nichols RA, Priestley JV, and Lummis SC (1999) Antibodies against the extracellular domain of the 5-HT3 receptor label both native and recombinant receptors. *Brain Res Mol Brain Res* **67:**221–230.
Spivak CE, Lupica CR, and Oz M (2007) The endocannabinoid anandamide inhibits the function of $\alpha4\beta2$ nicotinic acetylcholine receptors. *Mol Pharmacol* **72:**1024–1032.
Sun H, Hu XQ, Moradel EM, Weight FF, and Zhang L (2003) Modulation of 5-HT3 receptor-mediated response and trafficking by activation of protein kinase C. *J Biol Chem* **278:**34150–34157.
Tecott LH, Maricq AV, and Julius D (1993) Nervous system distribution of the serotonin 5-HT3 receptor mRNA. *Proc Natl Acad Sci U S A* **90:**1430–1434.
van Hooft JA, van der Haar E, and Vijverberg HP (1997) Allosteric potentiation of the 5-HT3 receptor-mediated ion current in N1E-115 neuroblastoma cells by 5-hydroxyindole and analogues. *Neuropharmacology* **36:**649–653.
Waeber C, Dixon K, Hoyer D, and Palacios JM (1988) Localisation by autoradiography of neuronal 5-HT3 receptors in the mouse CNS. *Eur J Pharmacol* **151:**351–352.
Waeber C, Hoyer D, and Palacios JM (1989) 5-hydroxytryptamine3 receptors in the human brain: autoradiographic visualization using [3H]ICS 205–930. *Neuroscience* **31:**393–400.
Waeber C, Pinkus LM, and Palacios JM (1990) The (S)-isomer of [3H]zacopride labels 5-HT3 receptors with high affinity in rat brain. *Eur J Pharmacol* **181:**283–287.
Yakel JL and Jackson MB (1988) 5-HT3 receptors mediate rapid responses in cultured hippocampus and a clonal cell line. *Neuron* **1:**615–621.
Zhang L and Lummis SC (2006) 5-HT3 receptors, in *Allosteric Receptor Modulation in Drug Targeting* (Bowery NG ed) pp 135–154, Taylor & Francis, New York.
Zimmer A, Zimmer AM, Hohmann AG, Herkenham M, and Bonner TI (1999) Increased mortality, hypoactivity, and hypoalgesia in cannabinoid CB1 receptor knockout mice. *Proc Natl Acad Sci U S A* **96:**5780–5785.

Address correspondence to: Dr. Li Zhang, Laboratory for Integrative Neuroscience National Institute on Alcohol Abuse and Alcoholism, National Institutes of Health, 5625 Fishers Lane, Bethesda, MD 20892. E-mail: lzhang@mail.nih.gov